Glycobiology, 2018, vol. 28, no. 11, 825–831
doi: 10.1093/glycob/cwy070
Advance Access Publication Date: 20 August 2018
Communication

OXFORD

Analytical Glycobiology

Glycosylation profiling of dog serum reveals differences compared to human serum

Anna-Janina Behrens[1,2], Rebecca M Duke[2], Laudine MC Petralia[2], David J Harvey[3,4], Sylvain Lehoux[5], Paula E Magnelli[2], Christopher H Taron[2], and Jeremy M Foster[1,2]

[2]New England Biolabs Inc., 240 County Road, Ipswich, MA 01938, USA, [3]Target Discovery Institute, Nuffield Department of Medicine, University of Oxford, Old Road Campus, OX3 7FZ, [4]Centre for Biological Sciences, Faculty of Natural and Environmental Sciences, University of Southampton, University Road, SO17 1BJ Southampton, UK, and [5]Department of Surgery, Beth Israel Deaconess Medical Center, Harvard Medical School, 330 Brookline Avenue, Boston, MA 02115, USA

[1]To whom correspondence should be addressed: Tel: +1 9789988948; e-mail: annaj.behrens@gmail.com (A.-J.B.); e-mail: foster@neb.com (J.M.F.)

Received 30 May 2018; Revised 16 July 2018; Editorial decision 16 July 2018; Accepted 30 July 2018

Abstract

Glycosylation is the most common post-translational modification of serum proteins, and changes in the type and abundance of glycans in human serum have been correlated with a growing number of human diseases. While the glycosylation pattern of human serum is well studied, little is known about the profiles of other mammalian species. Here, we report detailed glycosylation profiling of canine serum by hydrophilic interaction chromatography-ultraperformance liquid chromatography (HILIC-UPLC) and mass spectrometry. The domestic dog (*Canis familiaris*) is a widely used model organism and of considerable interest for a large veterinary community. We found significant differences in the serum *N*-glycosylation profile of dogs compared to that of humans, such as a lower abundance of galactosylated and sialylated glycans. We also compare the *N*-glycan profile of canine serum to that of canine IgG – the most abundant serum glycoprotein. Our data will serve as a baseline reference for future studies when performing serum analyses of various health and disease states in dogs.

Key words: glycan profiling, glycomics, glycosylation, *N*-glycans, serum

Introduction

The domestic dog (*Canis familiaris*) is a widely used animal model for a variety of human diseases like Alzheimer's, cancer, Duchenne muscular dystrophy (Shearin and Ostrander 2010; Barthélémy et al. 2012; Head 2013; Villarnovo et al. 2017; Gustafson et al. 2018) as well as for the experimental infection of human pathogens (Binhazim et al. 1993; Cerri et al. 1994). Dogs are commonly utilized in toxicology studies (Selvaraj et al. 2017; Sun et al. 2018) and, furthermore, there is a large veterinary interest surrounding the diagnosis and treatment of canine diseases.

Serum is an easily sampled body fluid that contains a high concentration of glycoproteins. Changes in the type and abundance of serum *N*- and *O*-glycans have been associated with a variety of different pathological states (Vanderschaeghe et al. 2009; Blomme et al. 2011; Xia et al. 2013; Saldova et al. 2014; Kirwan et al. 2015). Thus, glycans are attractive as a potential new class of diagnostic biomarkers. While there is in-depth understanding of human serum glycosylation, the literature on serum glycosylation profiles in other mammalian species is more limited. Multiple studies have analyzed *N*-glycan structures derived from IgG isolated from various

mammals and shown significant species-specific differences in the type and abundance of the observed *N*-glycans (Hamako et al. 1993; Raju et al. 2000; Adamczyk et al. 2014). However, studies addressing the composition of total serum *N*-glycomes in non-human mammals are needed, especially for animals widely used as model organisms.

Several studies have extensively characterized the *N*- and *O*-glycosylation of proteins in human blood serum using both mass spectrometry- and high/ultraperformance liquid chromatography (H/UPLC)-based workflows (Ruhaak et al. 2008; Aldredge et al. 2012; Xia et al. 2013; Saldova et al. 2014; Yabu et al. 2014; Stockmann et al. 2015). The most abundant glycoprotein in human serum is immunoglobulin G (IgG), which carries a variety of *N*-glycan structures in its Fc region. These structures are predominantly complex biantennary glycans containing zero, one or two terminal galactoses (Kobata 2008). Other than the immunoglobulins, all major serum glycoproteins such as transferrin, α2-macroglobulin, α1-antitrypsin, α1-acid glycoprotein, C3 complement and haptoglobin are synthesized in the liver (Miller and Bale 1954). Their hepatocyte-derived *N*-glycans generally dominate the total *N*-glycosylation profile of human serum (Aldredge et al. 2012). These *N*-glycans are frequently sialylated multiantennary structures (Vanderschaeghe et al. 2009; Blomme et al. 2011). Hence, the most abundant *N*-glycan in healthy human serum is a disialylated glycan A2G2S2 (Stockmann et al. 2015) (Figure 1; for a description of the glycan nomenclature see legend Table SI). In comparison to *N*-glycans, human serum *O*-glycans are structurally less complex. About 90% of the total *O*-glycan pool is comprised of core 1 (T antigen; Galβ1-3GalNAc), monosialylated core 1 (Neu5Acα2-3Galβ1-3GalNAc) and disialylated core 1 (Neu5Acα2-3Galβ1-3(Neu5Acα2-6)GalNAc) structures, with monosialylated core 1 being the most abundant *O*-glycan in healthy human serum by far (Xia et al. 2013; Yabu et al. 2014).

Here, we present the *N*-glycosylation profiling of healthy dog serum using hydrophilic interaction chromatography (HILIC)-UPLC and mass spectrometry as well as the analysis of both *N*- and *O*-glycans by matrix-assisted laser desorption/ionization time-of-flight mass spectrometry (MALDI-TOF MS). We show that there are marked differences in the abundance and structural composition of serum *N*-glycans from dogs in comparison to those of humans. Our study aims to provide a baseline dog serum *N*-glycome that can serve as an initial reference point for investigation of serum glycosylation changes in canine disease.

Results

Characterization of canine serum *N*-glycans

We performed HILIC-UPLC experiments in combination with fluorescence or mass spectrometry detection to analyze enzymatically released canine serum *N*-glycans. Glycan structures in the HILIC-UPLC profile (Figure 2A; Table SI) were assigned based on the susceptibility of individual glycans to sequential and individual, non-sequential exoglycosidase digests (Figure S1, Figure 3), based on their *m/z* values in the LC-ESI MS run (Table SI; due to the similarity of the HILIC columns used for UPLC and LC-ESI MS separation, *N*-glycans eluted at very similar relative retention) and on known mammalian *N*-glycosylation pathways. We assessed the coefficient of variation for the employed labeling method and subsequent analysis by HILIC-UPLC to be less than 15% for all peaks but one (Figure S2). We also investigated the impact of biological variation by analyzing the sera of five healthy dogs using the same method. As shown in Figure S3, all five biological replicates yielded highly similar spectra with very little variance.

N-glycan structures were additionally determined by total mass using MALDI-TOF MS of permethylated *N*-glycans in positive mode and by ion mobility LC-ESI MS of unlabeled glycans in negative mode (Figure 2B; Table SII; Table SIII). All three strategies yielded very similar and complementary information about the *N*-glycans of canine serum. The most abundant *N*-glycan comprising about 50% of the total glycan pool is the biantennary A2G2S2 glycan, followed by FA2G2 (~13%). As evident in Figure 3C, the majority of the *N*-glycans contain one or more terminal sialic acids

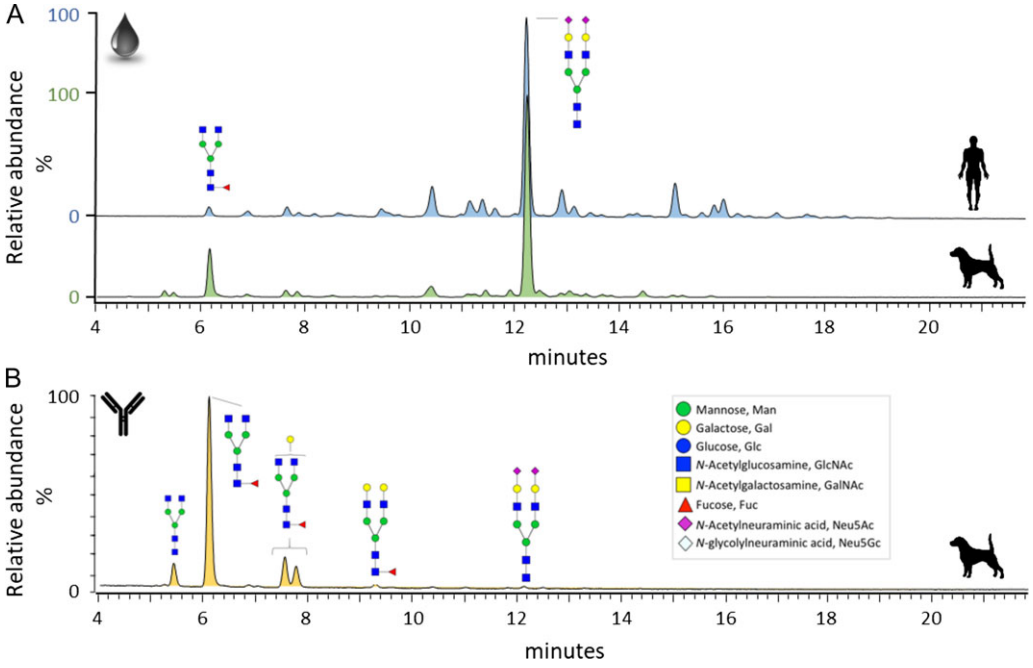

Fig. 1. (**A**) HILIC-UPLC profiles of enzymatically released and procainamide-labeled *N*-glycans from human (blue, top) and canine (green, bottom) blood serum. (**B**) HILIC-UPLC profile of *N*-glycans released from canine IgG. IgG was purified using Protein G from canine serum. Glycan structures are annotated following the nomenclature outlined by the Consortium for Functional Glycomics (CFG). The inset in B shows the monosaccharide symbols.

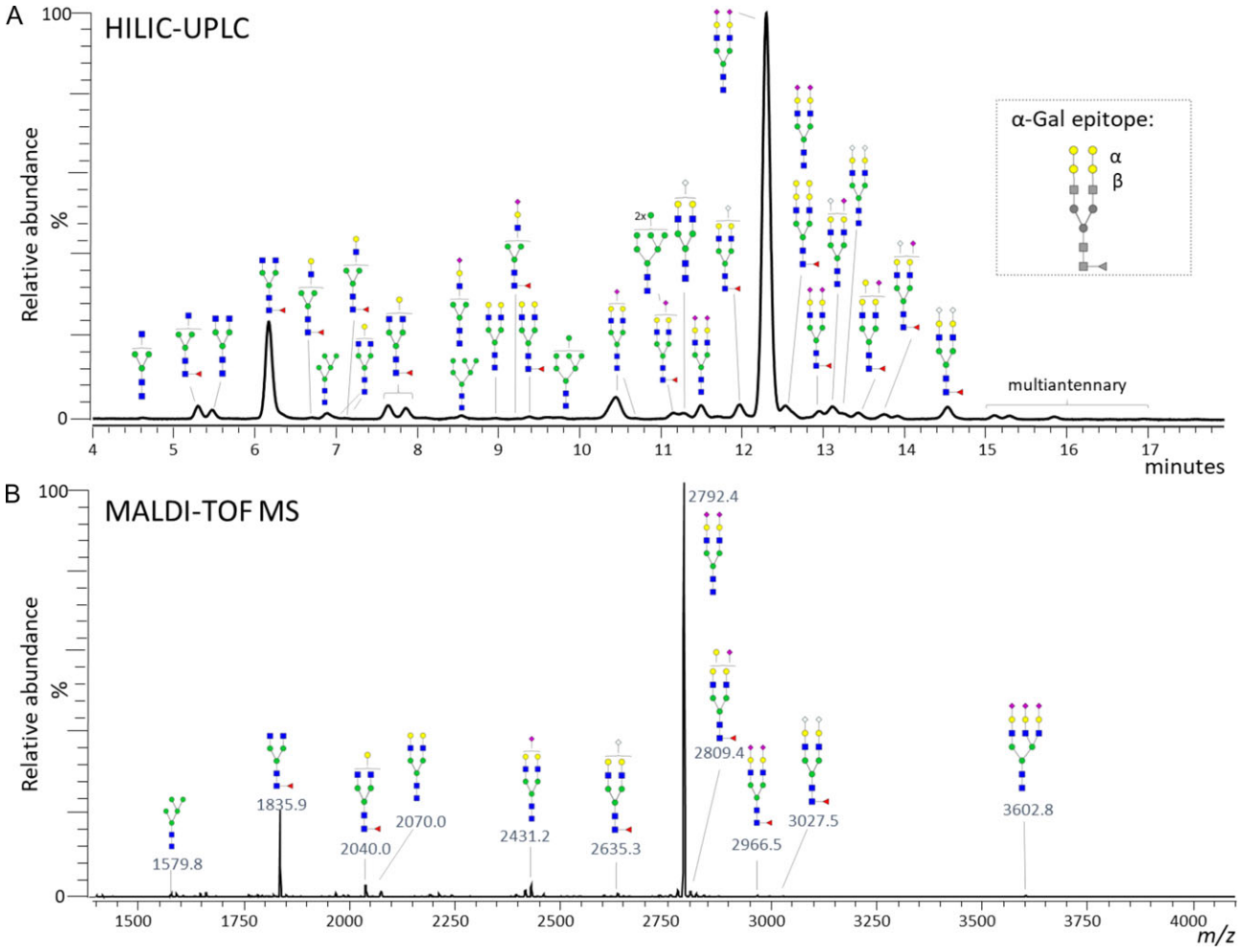

Fig. 2. *N*-glycosylation profile of canine serum. (**A**) HILIC-UPLC profile of procainamide-labeled *N*-glycans released from dog serum. See also Table SI. Glycan structures were confirmed by exoglycosidase digestions (Figure S1). (**B**) MALDI-TOF MS spectrum of enzymatically released and permethylated *N*-glycans from canine serum. See also Table SII. All molecular ions are $[M+Na]^+$. Monosaccharide codes as in inset Figure 1B.

(both Neu5Ac and Neu5Gc) – most of them are α2-6 linked (Figure S1). Additionally, we find evidence for the presence of the immunogenic α1-3-linked galactose (α-Gal) epitope (Figure 2A, inset; Figure S1).

In order to compare the total canine serum *N*-glycome to that of IgG – the most abundant serum glycoprotein, we purified IgG from canine serum using Protein A and Protein G magnetic beads and analyzed the *N*-glycans (Figure 1B). We note that the choice of either Protein A or Protein G for IgG purification does not impact the resulting *N*-glycan profile. Canine IgG predominantly carries *N*-glycans with zero, one or two terminal galactoses with FA2 being the most abundant *N*-glycan (~67%, Table S1). Interestingly and somewhat contrary to what has been reported previously (Adamczyk et al. 2014), we do not find any evidence – neither by mass spectrometry nor by HILIC-UPLC – for the presence of any bisecting *N*-glycans in canine serum and canine IgG.

The *N*-glycosylation profiles of dog and human serum are significantly different

The most expected difference of the canine and human serum *N*-glycomes is the presence in dog serum of the two well-known glycan epitopes that humans are usually not capable of generating – α-Gal and Neu5Gc (Figure 2A). A2G2S2 is the dominant glycan structure in both human as well as canine serum *N*-glycan profiles (Figure 1A). However, while the canine *N*-glycan profile has a large abundance of FA2, humans show a higher diversity of additional glycan structures with significant abundance.

We aimed to highlight differences in serum glycosylation between the two species by analyzing the abundance of three glycan classes (core fucosylation, terminal β-galactoses and terminal sialic acids; Figure 3). The relative abundance of each glycan class in the total pool of serum *N*-glycans was determined by exoglycosidase digestion of healthy canine ($n = 5$) and healthy pooled human ($n = 4$) serum. Compared to human serum, canine serum contains significantly more core fucosylated glycans (29% vs. 24%) and significantly fewer glycans carrying terminal galactoses and sialic acids (14% vs. 20%; 75% vs. 87%). The higher abundance of core fucosylated glycans can likely be explained by the intensity of the FA2 glycan peak in canine serum.

Analysis of canine serum *O*-glycans by MALDI-TOF MS

Additionally, we performed *O*-glycosylation profiling of canine blood serum by MALDI-TOF MS and MS/MS. Samples were

treated with PNGase F to remove the *N*-glycans followed by *O*-glycan release via reductive elimination and subsequent permethylation. The most abundant *O*-glycan in canine serum is the monosialylated core 1 structure $Neu5Ac_1Gal_1GalNAc_1$ (*m/z* 895.5), followed by the disialylated core 1 structure $Neu5Ac_2Gal_1GalNAc_1$ (*m/z* 1256.6; Figure 4). We were also able to identify masses that correspond to mono- and disialylated core 2 structures (*m/z* 1344.7 and *m/z* 1705.1). These results are similar to what has previously been reported for *O*-glycosylation of human serum (Xia et al. 2013; Yabu et al. 2014), except that we did not find any evidence for the presence of the T antigen. Further, we also did not see peaks corresponding to *O*-glycans containing Neu5Gc.

Discussion

In recent years numerous studies have described the repertoire of glycans that circulate on glycoproteins in serum and how they change in response to physiological changes brought on by healthy aging, lifestyle choices and disease. The hope is that glycans may one day be informative diagnostic biomarkers. To date, much of the work on serum glycomics has been performed with human blood and less is known about the composition of the serum glycome from other mammals. In this study, we defined the *N*-glycosylation and *O*-glycosylation profiles of healthy dog serum.

Compared to the human serum *N*-glycome, the abundance of fucosylated, biantennary, agalactosylated FA2 glycan was significantly more prominent in dogs (Figure 1A). It has previously been reported that the main contributor of FA2 abundance in human serum is IgG (Clerc et al. 2016). It has also been shown that canine and human IgG Fc glycosylation differ with respect to FA2 abundance, with about 50% of dog IgG *N*-glycans consisting of FA2 compared to 20% in humans (Adamczyk et al. 2014). Our analysis of canine IgG (Figure 1B) shows an even higher abundance of FA2 (67%). This observation might account for most of the differences

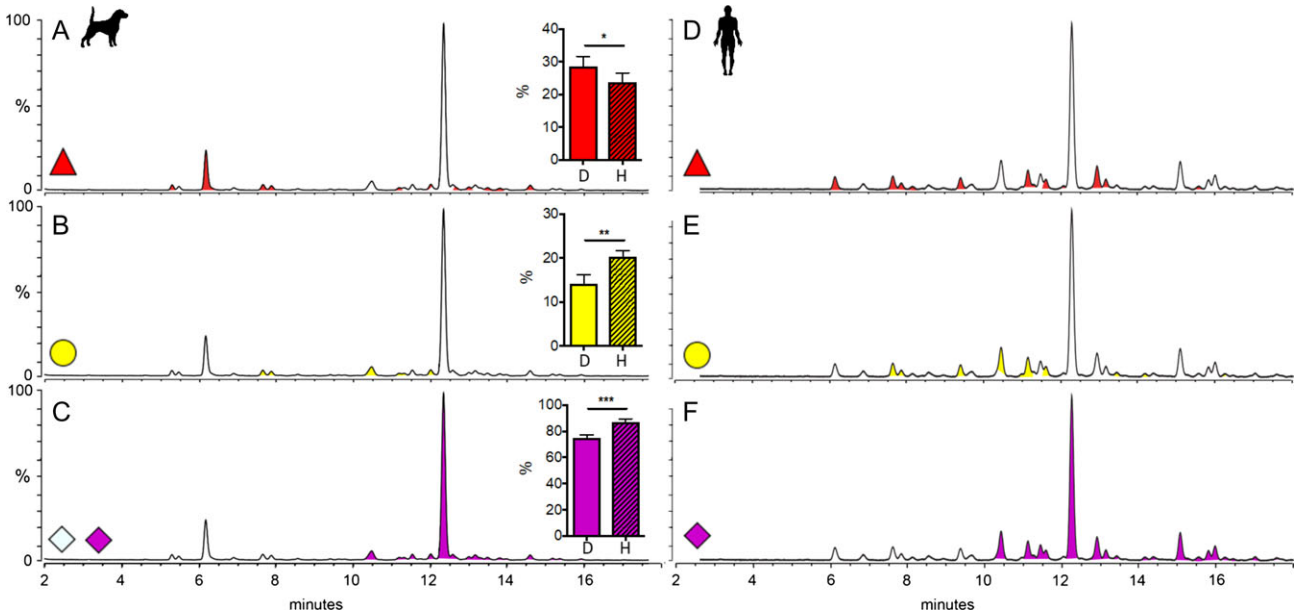

Fig. 3. Quantification of glycan classes of canine and human serum *N*-glycans. Representative HILIC-UPLC spectra of canine (left) and human (right) serum *N*-glycans are shown. The relative abundances of glycans containing core fucosylated (red; **A**, **D**), free terminal β-galactoses (yellow; **B**, **E**) or sialic acids (pink; Neu5Ac and Neu5Gc – **C**, Neu5Ac – **F**) were determined by quantification of spectra before and after digestion with Fucosidase O, β1-4 Galactosidase and Neuraminidase, respectively. The bar graphs compare the relative abundances of dog (D) and human (H) serum. The error bars show mean + SD from the analysis of $n = 5$ (canine serum samples; see Figure S3) and $n = 4$ (pooled human serum samples) biological replicates. Significances were determined by performing an unpaired *t*-test (fucosylation, $P = 0.0481$; galactosylation, $P = 0.0016$; sialylation, $P = 0.0002$).

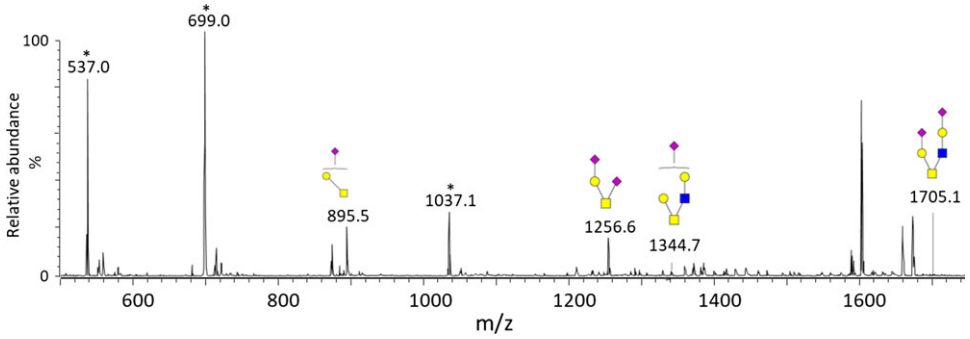

Fig. 4. MALDI-TOF MS of permethylated *O*-glycans isolated from canine serum. Glycans were released by reductive β-elimination, permethylated and analyzed by MALDI-TOF MS. All molecular ions are $[M+Na]^+$. Asterisk denotes known matrix peaks.

between the total serum *N*-glycan profiles for these two mammals. We also observe a lower abundance of *N*-glycans with terminal galactoses in canine serum. Galactosylation of plasma glycoproteins has been connected with blood clearance due to binding to the asialoglycoprotein receptor, which recognizes exposed galactose and *N*-acetylgalactosamine residues (Weigel 1994). The lower abundance of galactosylated *N*-glycans in canine serum could hint towards slight differences in blood glycoprotein homeostasis between humans and dogs.

Moreover, we observe interesting differences in the occurrence of two types of sialic acid, Neu5Ac and Neu5Gc. Prior studies on IgG from different mammalian species have revealed different patterns of Neu5Ac and Neu5Gc occurrence. For example, human and chicken IgG have been reported to exclusively contain Neu5Ac, whereas rhesus monkey, cow, sheep, goat and horse IgG contain only Neu5Gc. In organisms such as dogs, guinea pigs, rats and rabbits, IgG contains both Neu5Ac and Neu5Gc (Raju et al. 2000). Our analysis of total canine serum *N*-glycosylation is in accordance with the prior IgG data, with both Neu5Ac and Neu5Gc being observed. Interestingly however, our *O*-glycan analysis of canine serum (Figure 4) shows no evidence of Neu5Gc in any of the observed *O*-glycan structures.

In summary, this study, helps to establish a baseline serum *N*-glycosylation profile for dogs, and sets the stage for further study of how the glycome of this model organism responds to physiological changes due to health and disease.

Materials and methods

Human and canine serum samples

Canine blood serum samples were obtained from five healthy beagle dogs (one female and four males), which were housed at the TRS Laboratories Inc. (Athens, GA). Pools of healthy human serum were obtained from Innovative Research Inc., Sigma-Aldrich, Corning and VWR Scientific. Serum samples were stored at −20°C.

Purification of IgG from canine serum

IgG was purified from canine serum using either Protein A or Protein G magnetic beads according to the manufacturers' instructions (New England Biolabs).

N-glycan release and labeling with procainamide

Rapid release of *N*-glycans from serum or IgG was performed using Rapid PNGase F (New England Biolabs) as recommended by the supplier. A 5 µL aliquot of serum (20 µg IgG) was mixed with 3 µL of water and 2 µL of Rapid PNGase F buffer (New England Biolabs). The mixture was incubated at 70°C for 10 min. 1 µL Rapid PNGase F was added and the mixture was incubated for 5 min at 50°C, followed by 10 min at 90°C.

Following deglycosylation, released glycans were directly labeled with procainamide in the same tube. Stock solutions of procainamide (550 mg/mL DMSO) and sodium cyanoborohydride (200 mg/mL H_2O) were kept at −20°C and thawed prior to use (reagents remained stable for several weeks and numerous freeze/thaw cycles). Fresh labeling solution was prepared by adding one volume of acetic acid to eight volumes of procainamide stock solution. Acidified procainamide (9 µL) was added to each deglycosylation reaction, followed by 12 µL of the sodium cyanoborohydride stock solution. The samples were incubated for 45 min at 65°C.

After labeling, acetonitrile was added to the glycan-labeling-mixture to a final concentration of 85%. Using a vacuum manifold, the samples were cleaned-up using HILIC plates (SNS-HIL, The Nest Group Inc.). The plates were activated with 50 mM ammonium formate, pH 4.4 for 15 min and equilibrated with 90% acetonitrile/10% 50 mM ammonium formate, pH 4.4. Samples were loaded to the plates, washed 10 times with 90% acetonitrile/10% 50 mM ammonium formate, pH 4.4 and fluorescently labeled glycans were eluted in 100 µL 50 mM ammonium formate, pH 4.4.

HILIC-UPLC of fluorescently labeled *N*-glycans

The procainamide-labeled *N*-glycans were analyzed by HILIC-UPLC with fluorescence detection on a Waters Acquity H-class instrument composed of a binary solvent manager, a sample manager and a fluorescence detector. Glycans were separated using an Acquity BEH Amide Column (130 Å, 1.7 µm, 2.1 mM × 150 mM; Waters) with 50 mM ammonium formate, pH 4.4 as solvent A and acetonitrile as solvent B. The separation was performed using a linear gradient of 70–53% solvent B at 0.56 mL/min for 25 min. Fluorescence was measured using an excitation wavelength of 310 nm and a detection wavelength of 370 nm. Data acquisition, processing and analysis was performed using Empower 3 software (Waters). Glucose units were assigned using a procainamide-labeled dextran ladder and a fifth-order polynomial distribution curve. Glycan structures were assigned by exoglycosidase sequencing of the labeled glycan pool as well as by LC-ESI MS profiling.

Exoglycosidase digestion of released glycans

Digestion of released glycans with a panel of recombinant exoglycosidases was performed to quantify the abundance of individual glycan classes (e.g., those carrying core fucoses) as well as to confirm glycan structures via sequential digestion. Glycans were digested with α2-3,6,8 Neuraminidase, α2-3 Neuraminidase, α1-2,4,6 Fucosidase O, β1-4 Galactosidase, β-N-Acetyl-Glucosaminidase, α1-2,3,6 Mannnosidase, α1-3,4,6 Galactosidase (all from New England Biolabs) according to the manufacturer's instructions, then extracted using a 96-well hydrophobic polyvinyl fluoride (PVDF) protein-binding membrane plate as recommended (Merck Millipore).

LC-ESI MS of *N*-glycans

LC-ESI MS profiling of procainamide-labeled glycans was performed using an UltiMate 3000 UHPLC (Thermo Fisher Scientific) equipped with an 8 µL fluorescent cell coupled to a LTQ Velos Pro (Thermo Fisher Scientific) mass spectrometer (see Supplementary methods). Unlabled glycans were also analyzed ion mobility LC-ESI MS analysis using an Agilent 6560 ion-mobility Q-TOF mass spectrometer fitted with a JetSpray electrospray ion source and operated in negative ion mode (see Supplementary methods).

Glycan release and permethylation

For glycomics experiments, *N*-linked glycans were first released from serum using Rapid PNGase F (New England Biolabs) as described in methods. They were separated from the serum proteins using a Sep-Pak C18 cartridge (50 mg; Waters). Cartridges were conditioned sequentially with methanol, 5% acetic acid, 1-propanol and 5% acetic acid. A 200 µL volume of 5% acetic acid was added to the Rapid PNGase F-digested serum sample and loaded onto the column. The column was washed with 1 mL of 5% acetic acid. The flow-through and wash fraction containing released *N*-glycans were

collected, pooled, lyophilized and permethylated. De-*N*-glycosylated proteins were eluted from the column using sequential elutions of 20%, 40% and 100% 1-propanol. Elution fractions were pooled and lyophilized. *O*-glycans were then released by reductive β-elimination as described previously by using 55 mg/mL $NaBH_4$ in 0.1 M NaOH (Stansell et al. 2011). *N*- and *O*-glycans were permethylated using sodium hydroxide as described previously (Stansell et al. 2015; Panico et al. 2016) and then subjected to MALDI-TOF MS and MS/MS analysis.

MALDI-TOF MS analysis of permethylated *N*- and *O*-glycans

MALDI-TOF MS and MS/MS data on permethylated glycans was acquired in reflectron positive ion mode using an UltraFlex II MALDI-TOF mass spectrometer (Bruker). Lyophilized samples were resuspended in 10 µL of 75% methanol of which 1 µL was mixed in a 1:1 (v/v) ratio with 2,5-dihydrobenzoic acid (DHB; 10 mg/mL in 50% methanol) as a matrix. Spectra were acquired using flexControl (Version 3.4; Bruker). At least 20000 laser shots were acquired and accumulated per sample over a mass range of 500–6000 Da for *N*-glycans and 500–2000 Da for *O*-glycans. Spectra were processed using mMass (Version 5.5.0; (Strohalm et al. 2008)). Glycan structures were assigned both manually and with the help of GlycoWorkbench (Damerell et al. 2015).

Supplementary data

Supplementary data is available at *Glycobiology* online.

Funding

We thank New England Biolabs for financial support. We also gratefully acknowledge the National Center for Research Resources (a part of the NIH) for support of the National Center for Functional Glycomics (NCFG) at Beth Israel Deaconess Medical Center (P41GM103694). The content of this work is solely the responsibility of the authors and does not necessarily represent the official views of the National Center for Research Resources or the NIH.

Conflict of interest statement

The authors declare that there are no conflicts of interest.

Abbreviations

HILIC-UPLC, hydrophilic interaction chromatography-ultraperformance liquid chromatography; HPLC, high performance liquid chromatography; IgG, immunoglobulin G; MALDI-TOF MS, Matrix-assisted laser desorption/ionization time-of-flight mass spectrometry; LC-ESI MS, liquid chromatography electrospray mass spectrometry; DHB, 2,5-dihydrobenzoic acid; ASGR, asialoglycoprotein receptor

References

Adamczyk B, Tharmalingam-Jaikaran T, Schomberg M, Szekrenyes A, Kelly RM, Karlsson NG, Guttman A, Rudd PM. 2014. Comparison of separation techniques for the elucidation of IgG N-glycans pooled from healthy mammalian species. *Carbohydr Res*. 389:174–185.

Aldredge D, An HJ, Tang N, Waddell K, Lebrilla CB. 2012. Annotation of a serum N-glycan library for rapid identification of structures. *J Proteome Res*. 11:1958–1968.

Barthélémy I, Uriarte A, Drougard C, Unterfinger Y, Thibaud J-L, Blot S. 2012. Effects of an immunosuppressive treatment in the GRMD dog model of duchenne muscular dystrophy. *PLoS One*. 7:e48478.

Binhazim AA, Chapman WL Jr., Shin SS, Hanson WL. 1993. Determination of virulence and pathogenesis of a canine strain of *Leishmania leishmania infantum* in hamsters and dogs. *Am J Vet Res*. 54:113–121.

Blomme B, Van Steenkiste C, Grassi P, Haslam SM, Dell A, Callewaert N, Van Vlierberghe H. 2011. Alterations of serum protein N-glycosylation in two mouse models of chronic liver disease are hepatocyte and not B cell driven. *Am J Physiol Gastrointest Liver Physiol*. 300:G833–G842.

Cerri D, Farina R, Andreani E, Nuvoloni R, Pedrini A, Cardini G. 1994. Experimental infection of dogs with *Borrelia burgdorferi*. *Res Vet Sci*. 57:256–258.

Clerc F, Reiding KR, Jansen BC, Kammeijer GS, Bondt A, Wuhrer M. 2016. Human plasma protein N-glycosylation. *Glycoconj J*. 33:309–343.

Damerell D, Ceroni A, Maass K, Ranzinger R, Dell A, Haslam SM. 2015. Annotation of glycomics MS and MS/MS spectra using the GlycoWorkbench software tool. In: Lütteke T, Frank M, editors. *Glycoinformatics*. New York: Humana Press. p. 3–15.

Gustafson DL, Duval DL, Regan DP, Thamm DH. 2018. Canine sarcomas as a surrogate for the human disease. *Pharmacol Ther*. 188:80–96.

Hamako J, Matsui T, Ozeki Y, Mizuochi T, Titani K. 1993. Comparative studies of asparagine-linked sugar chains of immunoglobulin G from eleven mammalian species. *Comp Biochem Physiol*. 106:949–954.

Head E. 2013. A canine model of human aging and Alzheimer's disease. *Biochim Biophys Acta*. 1832:1384–1389.

Kirwan A, Utratna M, O'Dwyer ME, Joshi L, Kilcoyne M. 2015. Glycosylation-based serum biomarkers for cancer diagnostics and prognostics. *Biomed Res Int*. 2015:490531.

Kobata A. 2008. The N-linked sugar chains of human immunoglobulin G: Their unique pattern, and their functional roles. *Biochim Biophys Acta*. 1780:472–478.

Miller LL, Bale WF. 1954. Synthesis of all plasma protein fractions except gamma globulins by the liver; the use of zone electrophoresis and lysine-epsilon-C14 to define the plasma proteins synthesized by the isolated perfused liver. *J Exp Med*. 99:125–132.

Panico M, Bouche L, Binet D, O'Connor MJ, Rahman D, Pang PC, Canis K, North SJ, Desrosiers RC, Chertova E et al. 2016. Mapping the complete glycoproteome of virion-derived HIV-1 gp120 provides insights into broadly neutralizing antibody binding. *Sci Rep*. 6:32956.

Raju TS, Briggs JB, Borge SM, Jones AJ. 2000. Species-specific variation in glycosylation of IgG: Evidence for the species-specific sialylation and branch-specific galactosylation and importance for engineering recombinant glycoprotein therapeutics. *Glycobiology*. 10:477–486.

Ruhaak LR, Huhn C, Waterreus WJ, de Boer AR, Neususs C, Hokke CH, Deelder AM, Wuhrer M. 2008. Hydrophilic interaction chromatography-based high-throughput sample preparation method for N-glycan analysis from total human plasma glycoproteins. *Anal Chem*. 80:6119–6126.

Saldova R, Asadi Shehni A, Haakensen VD, Steinfeld I, Hilliard M, Kifer I, Helland A, Yakhini Z, Borresen-Dale AL, Rudd PM. 2014. Association of N-glycosylation with breast carcinoma and systemic features using high-resolution quantitative UPLC. *J Proteome Res*. 13:2314–2327.

Selvaraj S, Oh JH, Spanel R, Langer F, Han HY, Lee EH, Yoon S, Borlak J. 2017. The pathogenesis of diclofenac induced immunoallergic hepatitis in a canine model of liver injury. *Oncotarget*. 8:107763–107824.

Shearin AL, Ostrander EA. 2010. Leading the way: Canine models of genomics and disease. *Dis Model Mech*. 3:27–34.

Stansell E, Canis K, Haslam SM, Dell A, Desrosiers RC. 2011. Simian immunodeficiency virus from the sooty mangabey and rhesus macaque is modified with O-linked carbohydrate. *J Virol*. 85:582–595.

Stansell E, Panico M, Canis K, Pang PC, Bouche L, Binet D, O'Connor MJ, Chertova E, Bess J, Lifson JD et al. 2015. Gp120 on HIV-1 virions lacks O-linked carbohydrate. *PLoS One*. 10:e0124784.

Stockmann H, O'Flaherty R, Adamczyk B, Saldova R, Rudd PM. 2015. Automated, high-throughput serum glycoprofiling platform. *Inegr Biol*. 7:1026–1032.

Strohalm M, Hassman M, Kosata B, Kodicek M. 2008. mMass dataminer: An open source alternative for mass spectrometric data analysis. *Rapid Commun Mass Spectrom*. 22:905–908.

Sun J, Niu YM, Zhang YT, Li HJ, Yin Y, Zhang YZ, Ma PB, Zhou J, Huang L, Zhang HS et al. 2018. Toxicity and toxicokinetics of *Amanita exitialis* in beagle dogs. *Toxicon*. 143:59–67.

Vanderschaeghe D, Laroy W, Sablon E, Halfon P, Van Hecke A, Delanghe J, Callewaert N. 2009. GlycoFibroTest is a highly performant liver fibrosis biomarker derived from DNA sequencer-based serum protein glycomics. *Mol Cell Proteomics*. 8:986–994.

Villarnovo D, McCleary-Wheeler AL, Richards KL. 2017. Barking up the right tree: Advancing our understanding and treatment of lymphoma with a spontaneous canine model. *Curr Opin Hematol*. 24:359–366.

Weigel PH. 1994. Galactosyl and N-acetylgalactosaminyl homeostasis: A function for mammalian asialoglycoprotein receptors. *Bioessays*. 16:519–524.

Xia B, Zhang W, Li X, Jiang R, Harper T, Liu R, Cummings RD, He M. 2013. Serum N-glycan and O-glycan analysis by mass spectrometry for diagnosis of congenital disorders of glycosylation. *Anal Biochem*. 442:178–185.

Yabu M, Korekane H, Miyamoto Y. 2014. Precise structural analysis of O-linked oligosaccharides in human serum. *Glycobiology*. 24:542–553.